FMCW SUBSURFACE MICROWAVE IMAGING WITH HEXAGONAL ANTENNA ARRAY

Vincent R. Radzicki
Faculty Advisor: Hua Lee
Department of Electrical and Computer Engineering
University of California, Santa Barbara

ABSTRACT

Ground-penetrating radar (GPR) imaging is typically conducted in the pulse-echo mono-static format with a simple CW pulse as the probing signal. Recently, the data-acquisition hardware has been extended to the use of linear multi-element arrays. This paper presents an advanced GPR imaging system with FMCW probing waveforms, with a seven-element hexagonal array and software-defined data-acquisition hardware. The use of FMCW probing signals is for the optimization of the information contents of the returned waveforms. The utilization of the hexagonal unit is to produce sub-images with direction-independent resolution capability. In this paper, mathematical analysis, system modeling, field experiments, and image reconstruction are included to illustrate the performance and capability of the engineering concepts.

INTRODUCTION

The objective of this research project is the design and implementation of a portable, low-power ground penetrating radar (GPR) imaging system, operating in the step-frequency FMCW mode. The data-acquisition device consists of a 7-element antenna array configured in a hexagonal geometry, where antennas will be at an equal distance to the adjacent elements, for the improvement of symmetry in cross-range resolution. The antenna array is driven by a fully programmable software-defined radar unit with operational bandwidth from 0.9 GHz to 2 GHz, in 1102 frequency steps. The corresponding range resolution in the subsurface region is *6.82* cm for the 1.1 GHz bandwidth.

This system can function as a solitary unit in the form of a simple microwave flashlight, producing 3D collimated cylindrical images of the subsurface region. The system can also function in the synthetic-aperture mode to produce the three-dimensional subsurface profile of a greater region. The redundancy from the 7-element array unit provides improved accuracy of estimation and compensation of the platform motion of the synthetic-aperture scan. In addition, the geometrical properties of the hexagonal structure minimize the degradation due to platform rotation from the nonlinear scan paths.

Multiple array units can also be combined to form a larger hexagonal imaging array. The nature of the hexagonal structure allows effective integration. The radial symmetry of the images due to the hexagonal configuration gives superior accuracy in 3D image registration during the superposition process. The geometrical properties of the hexagonal structure are retained during the image reconstruction and superposition procedures.

HARDWARE COMPONENTS

The hardware used for the ground penetrating radar imaging system consists of three main components of (1) the radar unit, (2) the transceiver antenna array, and (2) a computer unit for the control and image formation of the system. The MIMO radar unit for this project is a programmable software-defined radar, with 8 user-defined input/output ports, and operating in the step-frequency FMCW mode. All transmission-waveform parameters, consisting of the frequency hopping rate, bandwidth, and frequency increment are selected by the user. The transmit power is 50mW, and the operating frequency range chosen for this experiment was 0.9 GHz to 2.0 GHz, corresponding to a total bandwidth of 1.1GHz. The system's frequency hopping rate can be programmed up to 90,000 hops per second. For this experiment, it was set at 15,000 hops per second to increase the observation period for improved data accuracy. The entire imaging radar is powered by a 12V DC input. Figure (1) shows the radar unit.

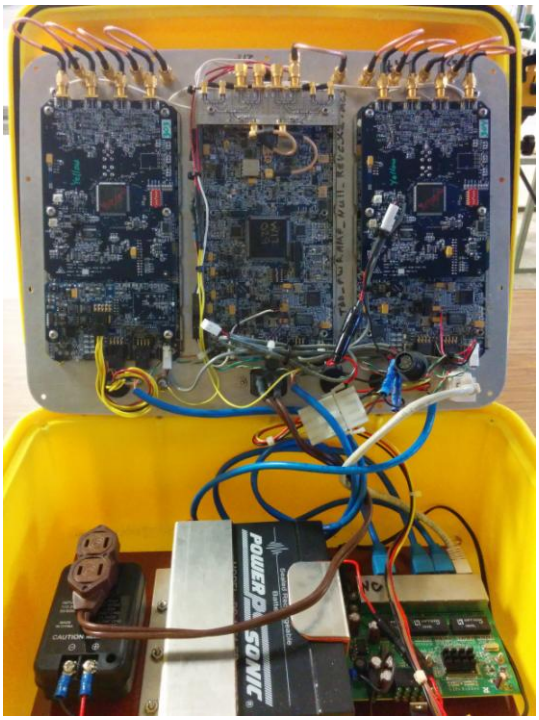

Figure (1): 8-port MIMO radar unit

The antenna array consists of 7 planar bow-tie antennas, organized in a hexagonal configuration, as shown in Figure (2). This configuration allows the resolution of the sub-images to be rotation independent. The spacing between antenna elements is set at 13.65 cm, making the dimension of the hexagonal array 30 cm x 30 cm. A metal plane was attached behind the antenna array and connected to a common ground to improve the directivity of the antennas. The transmitting element is at the center of the hexagonal array. At each data-acquisition position, the centered antenna transmits and the six surrounding antennas act as receivers. So, at each position, the array produces six tracks of data sequences, corresponding to one single transmitter.

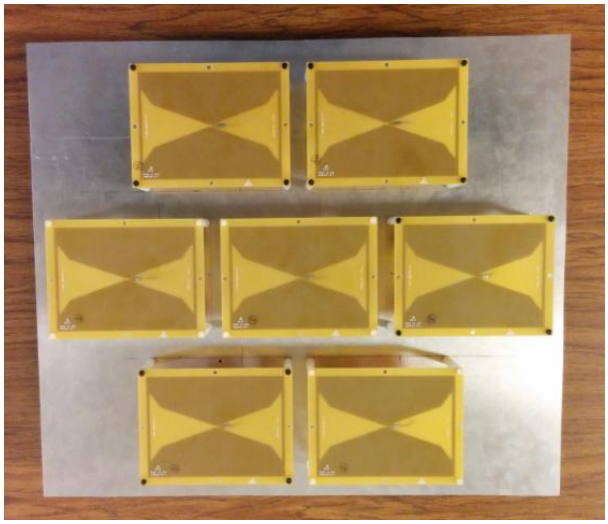

Figure (2) Hexagonal antenna array unit

RANGE ESTIMATION AND IMAGE RECONSTRUCTION

The first step in the image reconstruction process is the formation of the range profile at the data-acquisition position. For conventional systems, the transmitted signals are typically a predefined pulse, known as the probing waveforms. The estimation of the range profiles can then be performed by correlating the received waveforms with the probing signal.

Employing step-frequency FMCW is an alternative probing technique. Instead of one single probing waveform, the step-frequency FMCW system transmits a sequence of coherent signals. These CW signals are within the frequency band B with frequency increment Δf

$$f = f_0 + k\,\Delta f \qquad \text{where } k = 0, 1, 2, \ldots N\text{-}1 \qquad (1)$$

where N is the total number of FMCW frequency steps. For simplicity, the transmitted signal can be written in the phasor form of,

$$s(t) = A\ exp(-j2\pi ft\ ) \qquad (2)$$

For a propagation distance r, the travel time is $\tau = r/v$ where v is the propagation speed. Then, responding to a single target, the reflected signal detected by the receiver is in the form of a weighted and delayed version of the transmitted waveform,

$$g(t) = \alpha\ A\ exp(-j2\pi f(t - \tau)) = \alpha\ A\ exp(-j2\pi f(t - r/v)) \qquad (3)$$

where α denotes the weighting is due to the target reflectivity and propagation loss, and the delay is due to the round-trip travel time, from the transmitter to the receiver. At each frequency step, after demodulation, the received signal becomes,

$$g(t)\ s^{*}(t) = \alpha\ |A|^2\ exp(j2\pi f\tau) \qquad (4)$$

$$= \alpha\ |A|^2\ exp(j2\pi f(r/v))$$

After the demodulation, for each frequency, the result is a complex scalar. Through the N frequency steps, a complete illumination cycle produces an N-point sequence $\{p(k)\}$ from the demodulated received waveforms.

$$p(k) = g(t)\ s^{*}(t) \qquad (5)$$

$$= \alpha\ |A|^2\ exp(j2\pi\ (f_0 + k\ \Delta f\ )(r/v))$$

$$= \alpha\ |A|^2\ exp(j2\pi f_0\ (r/v))\ exp(j2\pi k\Delta f\ (r/v))$$

The term $exp(j2\pi k\Delta f\ (r/v))$ is the only one as a function of the index k. Then we match the core part of the sequence against the kernel of the FFT operator

$$exp(j2\pi k\Delta f\ (r/v)) = exp(j2\pi nk/N) \qquad (6)$$

The matching results in a simple relationship,

$$\frac{n}{N} = \left(\frac{\Delta f}{v}\right) r \tag{7}$$

It is then simplified down to a linear relationship between the *FFT* index *n* and the propagation distance *r*,

$$\textit{propagation distance} = r = \left(\frac{v}{B}\right) n \tag{8}$$

where *B* is the bandwidth of the waveform, defined as $B = N\Delta f$. Thus, the estimation of the range profile from the step-frequency FMCW system can be achieved with a simple *FFT* operator. Since the index *n* is an integer, the scaling factor $\frac{v}{B}$ represents the increment of the range profile, which is often referred to as the range resolution,

$$\textit{resolution in range direction} = \Delta r = \frac{v}{B} \tag{9}$$

The hexagonal-array unit operates in the bi-static mode, with one centered transmitter and six neighboring receivers. At each data-acquisition position, six tracks of FMCW data sequences are collected. Six range profiles are then calculated through Fourier transformation operations. The average of these six range profiles produces the range profile corresponding to the center of the hexagonal array. In combination, at each scan position, there exists a 7-track collimated hexagonal range profile. This approach can be described as the strip-mapping method that a target profile along the depth direction is estimated at each data-acquisition position.

Equal weighting is utilized for the standard hexagonal arrays, for the equal distance between adjacent antenna elements. For hexagonal arrays with non-uniform spacing, difference weighting schemes are then applied.

EXPERIMENTS AND RESULTS

Laboratory experiments were conducted to verify the mathematical analysis and physical modeling. The experiments were used to document the accuracy of the image reconstruction algorithm and evaluate the performance of the overall system. As shown in Figure (3), the test apparatus include an electronically controlled mechanical scanning system over a large test bed. For simplicity, dry sand is used as the propagation medium for homogeneity. The indoor test

apparatus allowed for controlled and consistent environmental conditions for the capacity of repeated data-acquisition exercises.

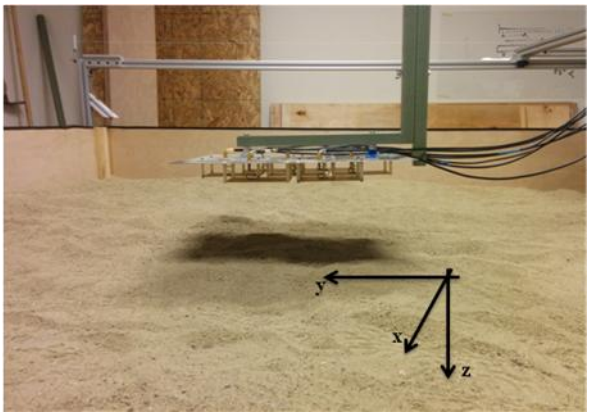

Figure (3) Antenna array mount to test apparatus

The operating frequency bandwidth of the transmission signal of the radar was selected to be 1.1 GHz with a hopping rate of 15,000 frequency hops per second. The total number of FMCW frequency steps is 1102 at each data-acquisition position.

The relative permittivity of the sand in the experiment is estimated to be $\varepsilon = 4$, which results in the wave propagation speed to be scaled down by a factor of $\sqrt{\varepsilon} = 2$. As a result, the range resolution of the surface region is $\Delta r = 6.82$ *cm.* A corner reflector was used as the target for the laboratory experiments, as shown in Figure (4). The subsurface depth of the reflector is approximately *12.7 cm.*

Figure (4): Corner reflector as target for subsurface imaging experiment

In these experiments, the data-acquisition system conducts a raster scan to form a two-dimensional aperture. A 512-count encoder tracks the vertical movement of the antenna array.

The multi-frequency backward propagation method, approximated in the form of Fourier transformation, is then used for the image reconstruction. The algorithm converted the raw data into a full three-dimensional image of the region of interest. Two-dimensional image slices can then be selected from the three-dimensional image volume for inspection.

A horizontal image slice of the region directly above the corner reflector, is shown in Figure (5). A vertical slice of the target region is shown in Figure (6).

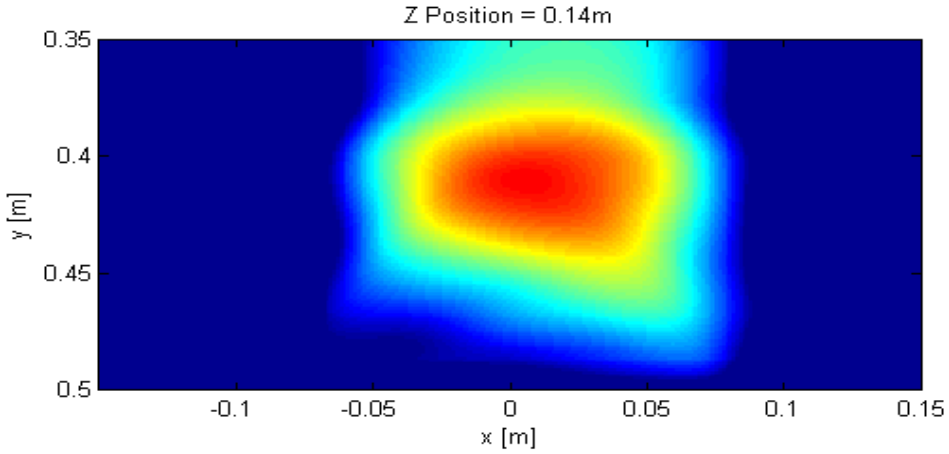

Figure (5): Horizontal planar cross-sectional image

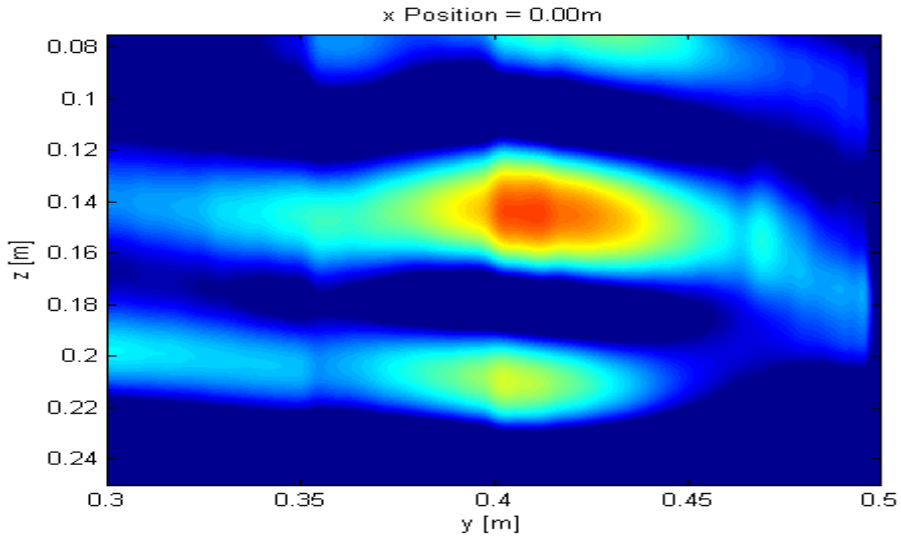

Figure (6): Vertical slice of the image of the target region

CONCLUSION

This paper presents the design and development of a portable, low-power, wideband, software-defined radar imaging system with a hexagonal antenna array and FMCW illumination. The use of FMCW waveforms for illumination enables the dynamic reconfiguration of the probing signal and Fourier transformation for the estimation of the range profiles with computation simplicity. The use of hexagonal array is to achieve uniform and direction-independent resolving capability. The presentation of this paper includes the design concepts, formulation of the range profiles and image formation, and laboratory subsurface-imaging experiments.

This system can be used as a single microwave imaging. Alternatively, it can function in the synthetic-aperture format to extend the aperture coverage to improve cross-range resolution. The objective applications in this paper are ground-penetrating radar imaging to demonstrate the capability of subsurface profiling. Nonetheless, the system can be easily applied to high-resolution imaging in-air or through-wall modalities.

REFERENCES

1. Hua Lee and Glen Wade, *Imaging Technology*, IEEE Press, New York, 1986.
2. H. Lee, "An Overview of Synthetic-Aperture Image Reconstruction Algorithms for GPR Imaging with Pulse-Echo and Step-Frequency FMCW Systems," *Journal of Environmental and Engineering Geophysics*, 8(2), pp. 105-114, June 2003.
3. Bretton L. Douglas and Hua Lee, "Synthetic-Aperture Active Sonar Imaging," *Proceedings of the 1992 IEEE International Conference on Acoustics, Speech, and Signal Processing*, pp. 37-40, Vol. III, 1992.
4. Bretton L. Douglas and Hua Lee, "Synthetic-Aperture Sonar Imaging with a Multiple Element Receiver Array," *Proceedings of IEEE International Conference on Acoustics, Speech and Signal Processing*, pp. V 445-448, 1993.
5. J. E. Mast, B. Edgar, T. W. Wall, J. P. Murtha, and Hua Lee, "Impulse Radar Imaging: Applications to Historic Buildings," *Proceedings of American Society for Nondestructive Testing Conference*, 1992.
6. Michael S. D'Errico, Bretton L. Douglas, and Hua Lee, "Subsurface Microwave Imaging for Nondestructive Evaluation of Civil Structures," *Proceedings of IEEE International Conference on Acoustics, Speech and Signal Processing*, pp. V 453-456, 1993.
7. Hua Lee and Joseph P. Murtha, "Pulse-Echo Microwave Tomographic Imaging and Object Recognition for NDE of Civil Structures and Materials," *Proceedings of the Second International Conference on Imaging Technologies: Techniques and Civil Engineering Applications*, 1997.
8. Mei-Su Wu and Hua Lee, "Remote Detection and Geolocation of Breathing Subjects by High-Performance Ultra-Wideband FMCW MIMO Microwave Imaging System," *Proceedings of International Telemetering Conference*, 2011.

9. Michael Lee, Daniel Doonan, Michael Liebling, and Hua Lee, "Resolution Analysis and System Integration of a Dynamically Reconfigurable FMCW Medical Ultrasound Imaging System," *Proceedings of International Telemetering Conference*, 2012.
10. Mei-Su Wu and Hua Lee, "Dynamically Reconfigurable Imaging with Flexible Transceiver Array and Programmable Probing Waveforms," *Proceedings of International Telemetering Conference*, 2013.
11. Michael Lee and Hua Lee, "Dynamic Acoustical Imaging Systems with Reconfigurable Transceiver Arrays and Probing Waveforms," *Program Summary of Annual Acoustical Society of America Meeting,* JASA, 134(5), p. 3997, 2013.
12. Michael Lee, Michael Liebling, and Hua Lee, "Modeling Imaging Performance of Multistatic Acoustic Arrays Non-uniform Geometries," *Program Summary of Annual Acoustical Society of America Meeting,* JASA, 134(5), p. 4170, 2013.